Kwan et al. BMC Structural Biology (2015) 15:18
DOI 10.1186/s12900-015-0043-3

BMC Structural Biology

RESEARCH ARTICLE Open Access

An intact helical domain is required for $G\alpha_{14}$ to stimulate phospholipase Cβ

Dawna HT Kwan[1], Ka M. Wong[1], Anthony SL Chan[1], Lisa Y. Yung[1] and Yung H. Wong[1,2*]

Abstract

Background: Stimulation of phospholipase Cβ (PLCβ) by the activated α-subunit of G_q ($G\alpha_q$) constitutes a major signaling pathway for cellular regulation, and structural studies have recently revealed the molecular interactions between PLCβ and $G\alpha_q$. Yet, most of the PLCβ-interacting residues identified on $G\alpha_q$ are not unique to members of the $G\alpha_q$ family. Molecular modeling predicts that the core PLCβ-interacting residues located on the switch regions of $G\alpha_q$ are similarly positioned in $G\alpha_z$ which does not stimulate PLCβ. Using wild-type and constitutively active chimeras constructed between $G\alpha_z$ and $G\alpha_{14}$, a member of the $G\alpha_q$ family, we examined if the PLCβ-interacting residues identified in $G\alpha_q$ are indeed essential.

Results: Four chimeras with the core PLCβ-interacting residues composed of $G\alpha_z$ sequences were capable of binding PLCβ2 and stimulating the formation of inositol trisphosphate. Surprisingly, all chimeras with a $G\alpha_z$ N-terminal half failed to functionally associate with PLCβ2, despite the fact that many of them contained the core PLCβ-interacting residues from $G\alpha_{14}$. Further analyses revealed that the non-PLCβ2 interacting chimeras were capable of interacting with other effector molecules such as adenylyl cyclase and tetratricopeptide repeat 1, indicating that they could adopt a GTP-bound active conformation.

Conclusion: Collectively, our study suggests that the previously identified PLCβ-interacting residues are insufficient to ensure productive interaction of $G\alpha_{14}$ with PLCβ, while an intact N-terminal half of $G\alpha_{14}$ is apparently required for PLCβ interaction.

Background

The superfamily of G protein-coupled receptors (GPCRs) constitutes the largest group of cell surface detectors for extracellular signals. Upon ligand binding, conformational changes in the receptor trigger the activation of heterotrimeric G proteins, which consists of α, β, and γ subunits, and results in the activation of various downstream effectors [1, 2]. Gα proteins are classified into four main families named as $G\alpha_s$, $G\alpha_i$, $G\alpha_q$, $G\alpha_{12/13}$, while five Gβ and twelve Gγ isoforms have been identified to date. The diversity in G protein subunits allows disparate signaling pathways to be regulated by different receptors. Robust stimulation of phospholipase Cβ (PLCβ) is primarily mediated by GPCRs that utilize $G\alpha_q$ proteins for signaling [3], thereby leading to diverse cellular responses that range from cell proliferation to differentiation. The four known isoforms of PLCβ (PLCβ1-4) [4] are all stimulated by GTP-bound $G\alpha_q$ subunits [5], even though they are either enriched in the cytosol (PLCβ2 and PLCβ3) or at the plasma membrane (PLCβ1 and PLCβ4) [6]. PLCβ catalyzes the hydrolysis of phosphatidylinositol 4,5-bisphosphate (PIP_2) into diacylglycerol and inositol 1,4,5-trisphosphate (IP_3), and reciprocally acts as a GTPase activating protein (GAP) of $G\alpha_q$ [7, 8]. Since there are several members within the $G\alpha_q$ subfamily ($G\alpha_q$, $G\alpha_{11}$, $G\alpha_{14}$, and $G\alpha_{15}$/$G\alpha_{16}$) and all are fully capable of stimulating PLCβ [5], numerous GPCRs employ the $G\alpha_q$/PLCβ pathway to regulate different cellular functions. Moreover, the Gβγ complex released upon G protein activation can also stimulate PLCβ2 and PLCβ3 isoforms [9, 10]. Given the importance of the $G\alpha_q$/PLCβ axis in cell growth [11], its dysregulation is expected to contribute to the pathophysiology of various diseases. Indeed, somatic mutations causing constitutive activation of $G\alpha_q$ drive ~50 % of all uveal melanomas [12].

* Correspondence: boyung@ust.hk
[1]Division of Life Science and the Biotechnology Research Institute, Hong Kong University of Science and Technology, Clear Water Bay, Kowloon, Hong Kong
[2]State Key Laboratory of Molecular Neuroscience, Hong Kong University of Science and Technology, Clear Water Bay, Kowloon, Hong Kong

Despite intense efforts directed at understanding the interactions of $G\alpha_q$ and PLCβ, the structure of a PLCβ-$G\alpha_q$ complex has only been recently solved by molecular replacement manipulations using the crystal structures of PLCβ3 and an activated $G\alpha_q$ [13]. The predicted structure of the PLCβ3-$G\alpha_q$ complex has identified a series of discrete residues that form the interacting surfaces (Fig. 1a). According to the structural data, PLCβ3 binding occurs mainly at the switch regions of $G\alpha_q$ (Fig. 1a and b). The switch I and II residues of $G\alpha_q$ (green) interact with PLCβ3 through an extended loop region between EF hands 3/4, which is conserved in all PLCβ isoforms (Additional file 1: Figure S1), and the region between the catalytic TIM barrel and C2 domain of PLCβ3, providing an interface between PLCβ3 and $G\alpha_q$ for interaction between a series of charged residue pairs. The highly conserved helix-turn-helix segment (Hα1/Hα2) at the C-terminus of the C2 domain of PLCβ3 resides on the surface region formed by switch II (α2-β4) and the α3 helix of $G\alpha_q$ and allows the formation of various contacts with $G\alpha_q$ in the large binding interface (Fig. 1c). More recently, discovery of the full-length structures of both PLCβ3 and $G\alpha_q$ in complex has highlighted additional domains of PLCβ3 and $G\alpha_q$ necessary for activation of lipid hydrolysis and protein interactions [14]. The crystallized full-length PLCβ3 contains a distal C-terminal domain (CTD) which is considered to be important for activation, membrane localization, and regulation by $G\alpha_q$ proteins [15, 16]. The distal CTD adopts an orientation that makes direct contacts with the αN helix of $G\alpha_q$ and most likely participates in binding with Gα proteins.

Regions of the $G\alpha_q$ necessary for PLCβ interaction (namely, Ile^{217} to Lys^{276} which encompass the α2-β4-α3-β5 regions) have previously been identified by alanine-scanning mutagenesis [17] and they are appropriately positioned for the interaction with PLCβ3 (Fig. 1a). A total of 33 amino acids in small clusters along the β2 to α4 regions (except Ile^{21}, Ile^{25}, and Leu^{29}, which lies in the αN helix, and Lys^{41} which lies on the β1 strand) of $G\alpha_q$ are predicted to form intermolecular bonds with PLCβ [13, 14]. As expected, most interacting residues in the core regions are conserved in all other $G\alpha_q$ members including $G\alpha_{11}$, $G\alpha_{14}$, and $G\alpha_{16}$ (Fig. 1a). However, between 36 and 60 % of the identified PLCβ-interacting residues are also found in other Gα protein families, with members of the $G\alpha_i$ family having the highest homology to $G\alpha_q$ (Additional file 1: Figure S2) [18, 19]. For instance, $G\alpha_z$ of the $G\alpha_i$ subfamily exhibits close to 60 % identity with $G\alpha_q$ in the core PLCβ-interacting regions (Fig. 1a). Such a high degree of identity is rather surprising especially when $G\alpha_{16}$, which stimulates PLCβ, is only 74 % identical to $G\alpha_q$ in the PLCβ-interacting regions (Fig. 1a). More interestingly, molecular modeling between $G\alpha_q$ and $G\alpha_z$ predicts that their differences in the PLCβ-interacting regions form a ring around a central core domain (Fig. 1b, space filled models), with most of the PLCβ contact points conserved between the two Gα subunits (Fig. 1c). This calls into question whether the residues identified by molecular replacement [13] are sufficient to provide PLCβ binding selectivity to $G\alpha_q$ members. Although the identified residues are involved in the formation of the PLCβ3-$G\alpha_q$ complex and are necessary in PLCβ3 activation as confirmed in IP_3 studies [13], there may be additional regions in $G\alpha_q$ members that determine selectivity for PLCβ.

It has been well established that constitutively active $G\alpha_q$ subunits can efficiently stimulate PLCβ [20] but has no regulatory effect on adenylyl cyclase [21]. Early studies have employed chimeric $G\alpha_q/G\alpha_s$ and $G\alpha_{16}/G\alpha_z$ constructs to map the PLCβ and receptor interacting domains on the $G\alpha_q$ and $G\alpha_{16}$ subunits [17, 22]. It has not been demonstrated whether other $G\alpha_q$ members such as $G\alpha_{14}$ (with over 80 % sequence similarity with $G\alpha_q$) utilize the same regions to interact with PLCβ. Likewise, it remains to be determined if other PLCβ isoforms such as PLCβ2 (with the highest resemblance to PLCβ3; Additional file 1: Figure S1) employ similar structural regions as PLCβ3 for coupling to active $G\alpha_q$. By generating a series of Gα subunit chimeras and testing their abilities to functionally associate with PLCβ2 in HEK293 cells, we have demonstrated that an intact helical domain in the N-terminus of $G\alpha_{14}$ is necessary for productive interaction with PLCβ.

Results

The PLCβ-interacting core regions of $G\alpha_{14}$ are insufficient to stimulate PLCβ2

The PLCβ-interacting surfaces of $G\alpha_q$ have been generally mapped to the β2-β3-α2-β4-α3 regions [13, 17], and these residues are mostly conserved among $G\alpha_{11}$, $G\alpha_{14}$, and $G\alpha_{16}$ (Fig. 1a). Given that most of the PLCβ contact sites of $G\alpha_q$ appear to be similarly present in $G\alpha_i$ subunits (Additional file 1: Figure S2), it is possible to confer PLCβ-stimulating function upon a $G\alpha_i$ subunit by incorporating $G\alpha_q$-specific residues. This will also allow for the identification of any additional structural determinant on $G\alpha_q$ which may specify interaction with PLCβ. In order to distinguish exogenous from endogenous Gα subunits, we have opted to use $G\alpha_{14}$ as the backbone for constructing chimeras instead of $G\alpha_q$ or $G\alpha_{11}$. Unlike $G\alpha_{q/11}$, $G\alpha_{14}$ is not expressed in HEK293 cells [23] and it differs from $G\alpha_q$ by only two amino acids (Lys^{256} and Thr^{296} in $G\alpha_{14}$) in the PLCβ-interacting regions (Fig. 1a, b). To determine if $G\alpha_{14}$ utilizes the same regions as $G\alpha_q$ for PLCβ interaction, $G\alpha_{14}/G\alpha_z$ chimeras were made by swapping specific domains between $G\alpha_{14}$ and $G\alpha_z$. $G\alpha_z$ was selected because it does not interact with PLCβ [24] or other $G\alpha_q$

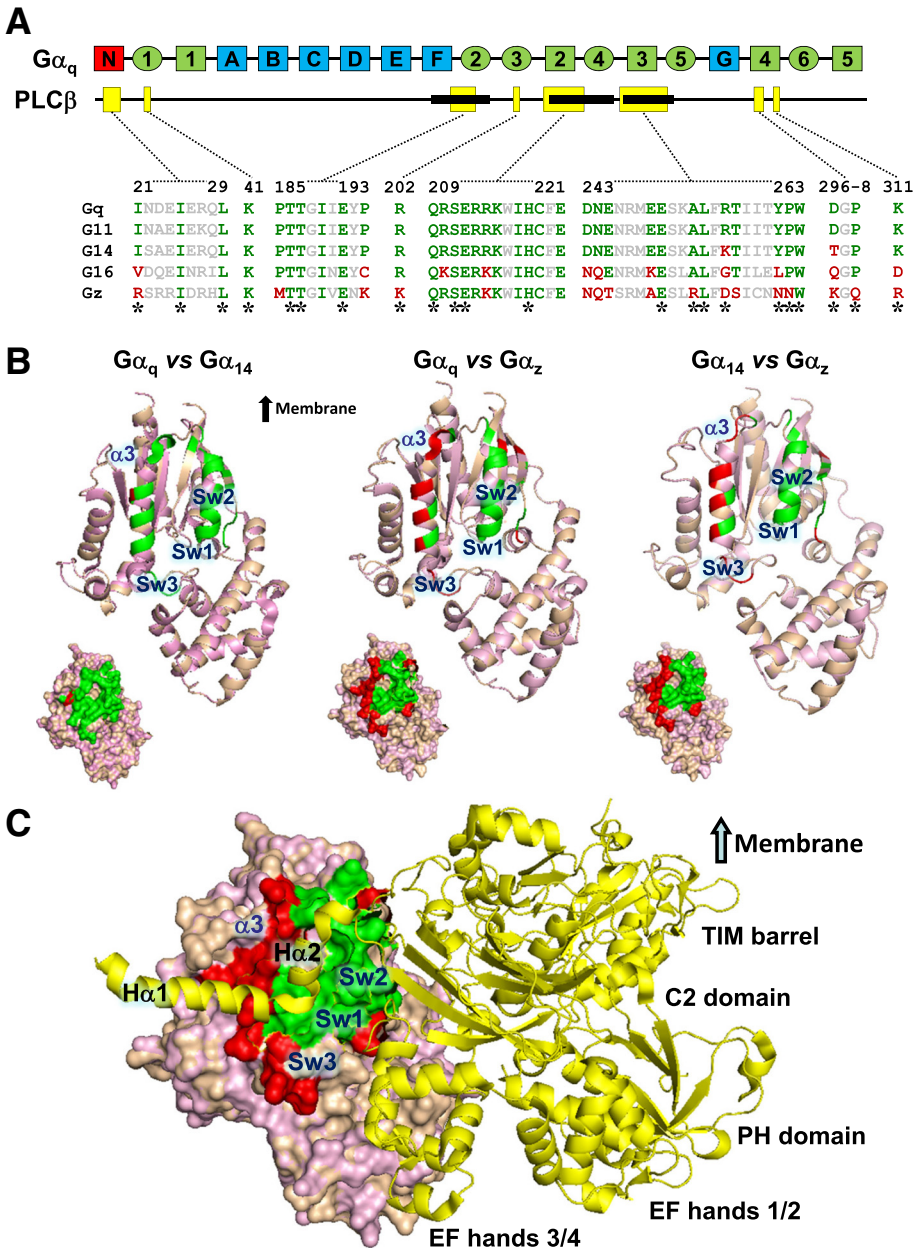

Fig. 1 Alignment of PLCβ-interacting residues in $G\alpha_q$ family and $G\alpha_z$. **a** Schematic view of $G\alpha_q$ divided into helical (light blue) and GTPase (light green) domains with α-helices and β-strands represented by rectangles and ovals, respectively. Interacting domains of $G\alpha_q$ with PLCβ are indicated by yellow boxes below the $G\alpha_q$ sequence; the three bold segments indicate the relative positions of the three switch regions (Sw1 to Sw3 from left to right). Sequence alignment of PLCβ-interacting domains in the $G\alpha_q$ family as compared to that of $G\alpha_z$; conserved (green) or divergent (red) PLCβ-interacting residues are interspersed by conserved residues which are not implicated in interaction with PLCβ (grey). Residues forming direct interactions with PLCβ3 as identified by Waldo *et al.* [13] are indicated by an asterisk. **b** Structural representation of $G\alpha_q$, $G\alpha_{14}$, and $G\alpha_z$ alignments with switch regions (Sw1-3) and the α3 region. PLCβ3-interacting residues revealed in the sequence alignment are colored as indicated in ***A***. Space filling models are showing interacting surfaces. Structural models of $G\alpha_{14}$ and $G\alpha_z$ are generated based on $G\alpha_q$-PLCβ3 (PDB code: 3OHM) using SWISS-MODEL [65, 66]. Structure alignments are carried out with PyMOL (The PyMOL Molecular Graphics System, Version 1.3 Schrödinger, LLC). **c** Complex of $G\alpha_q$/$G\alpha_z$-PLCβ3. The $G\alpha_q$/$G\alpha_z$ aligned model is represented as indicated in (B). PLCβ3 (yellow) is depicted as a cartoon ribbon, containing the helix-turn-helix segment (Hα1/Hα2), the N-terminal PH domain, four EF hands, the catalytic TIM barrel, and a C2 domain. The switch regions of $G\alpha_q$ interact with PLCβ3 through an extended loop region between EF hands 3/4 and the region between the catalytic TIM barrel and C2 domain. The helix-turn-helix segment (Hα1/Hα2) at the C-terminus of PLCβ3 resides on the surface region formed by switch 2 and α3 of $G\alpha_q$. The α_N helix of Gα proteins and carboxy-terminal (CT) domain of PLCβ3 are not included in the structural models

effectors such as TPR1 [25]. The chimeric approach is well suited for mapping functional domains on the Gα subunits because their tertiary structures highly resemble one another. Moreover, chimeras made with $G\alpha_z$ and $G\alpha_{16}$ proteins are structurally viable [22, 25].

Molecular modeling predicts that the differences between $G\alpha_{14}$ and $G\alpha_z$ in the PLCβ-interacting regions are distributed at the perimeters of the interacting surfaces, in much the same way as those of $G\alpha_q$ versus $G\alpha_z$ (Fig. 1b). Since most of the $G\alpha_z$-specific sequences in the PLCβ-interacting domain reside in the α2-β4-α3 regions (Fig. 1a), we began by testing the importance of these regions by swapping the C-terminal half of $G\alpha_z$ with $G\alpha_{14}$ and assaying for the ability of the chimeras to interact with PLCβ2; PLCβ2 was chosen on the basis that it shares 76 % identity with PLCβ3 at the $G\alpha_q$-interacting residues [13, 14]. The 14z151 chimera was constructed with the α2-β4-α3 regions together with the rest of the C-terminus of $G\alpha_{14}$ (151 residues) replaced by the cognate sequence from $G\alpha_z$; the mirror image of 14z151 was also constructed and named as 203z14 (Fig. 2a). Construction of the chimeras was guided by the predicted tertiary structure of the Gα subunits as well as by our previous experience in determining the receptor and effector interacting domains of various Gα subunits [22, 26–28]. A glutamine to leucine point mutation (QL) was introduced at Gln^{205} (equivalent to Gln^{209} in $G\alpha_q$) to generate constitutively active mutants [29]. HEK293 cells were co-transfected with PLCβ2 in combination with pcDNA1, wild-type or constitutively active mutant of $G\alpha_{14}$, $G\alpha_z$, 14z151 or 203z14. As illustrated in Fig. 2b (upper panels), wild-type and constitutively active $G\alpha_{14}$, but not those of $G\alpha_z$, were successfully co-immunoprecipitated by anti-

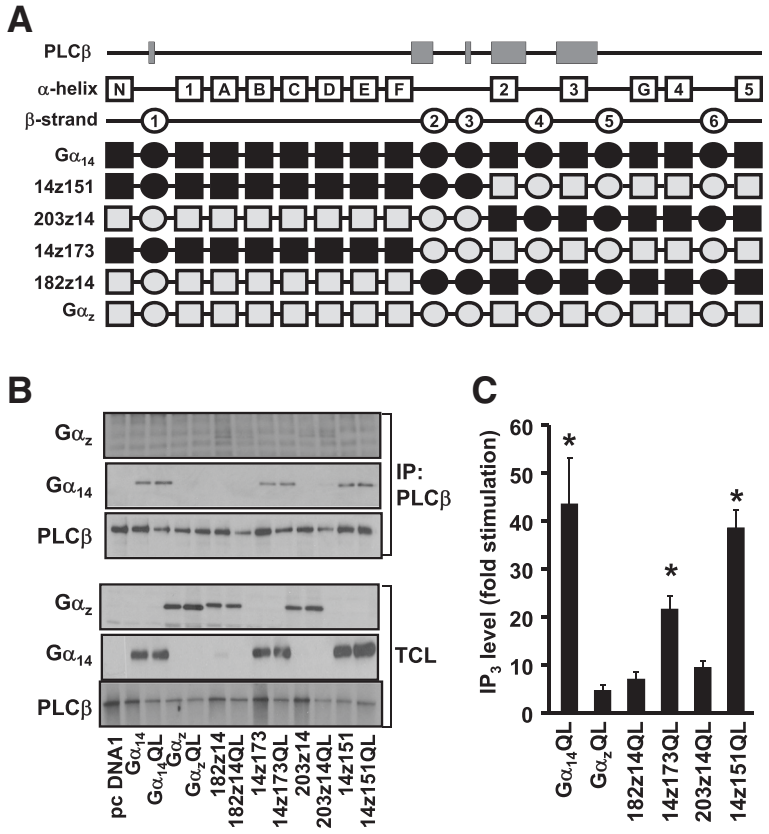

Fig. 2 The putative PLCβ domain of $G\alpha_{14}$ is not required for PLCβ interaction and activation. **a** Schematic representation of the 14z151, 203z14, 14z173, and 182z14 chimeras. Predicted secondary structures are illustrated as boxes (α helices) or circles (β strands) above the chimeras. Black areas represent human $G\alpha_{14}$ sequence while those in grey signify the corresponding sequence of human $G\alpha_z$. **b** HEK293 cells were co-transfected with PLCβ2 and the indicated Gα protein or chimeras. Cell lysates from the transfectants were immunoprecipitated by anti-PLCβ2 antiserum. The immunoprecipitates were immunoblotted with anti-$G\alpha_{14}$, anti-$G\alpha_z$ or anti-PLCβ2 antiserum. Aliquots of cell lysates were used to detect the expression levels of $G\alpha_{14}$, $G\alpha_z$ and PLCβ by Western blot analysis (TCL). Data shown represent one of three sets of immunoblots; two other sets yielded similar results. **c** HEK293 cells were transiently transfected with wild-type or constitutively active mutants (QL) of Gα protein or chimeras. Cells were then labelled and assayed for IP_3 formation. Fold stimulations were calculated as the ratios of QL-induced to wild-type IP_3 accumulations. Data represent the mean ± S.E.M. of three independent experiments, $n = 3$. *, IP_3 production was significantly enhanced as compared to corresponding wild-type transfected cells; Dunnett t test, $p < 0.05$

PLCβ2 antiserum and protein G sepharose. Chimera 203z14 did not interact with PLCβ2 despite having the α2-β4-α3 regions of $G\alpha_{14}$ (Fig. 2b). This indicates that the other PLC-interacting regions of $G\alpha_{14}$ (e.g., β2 and β3 regions) might be required for PLCβ2 interaction. More surprisingly, 14z151 was pulled down by anti-PLCβ2 even though its α2-β4-α3 regions were composed of $G\alpha_z$ sequences.

To test the possibility that the β2-β3 regions are needed to maintain the overall structural integrity of the PLCβ-interacting surfaces, we further constructed a pair of chimeras with the junction extended forward to include the β2-β3 regions (Fig. 2a). Again, both the wild-type and constitutively active mutant of the chimera which harbored the β2-β3-α2-β4-α3 regions of $G\alpha_{14}$ (182z14 and 182z14QL) failed to associate with PLCβ2, while their mirror images (14z173 and 14z173QL) co-immunoprecipitated with PLCβ2 (Fig. 2b). All of the chimeras and PLCβ2 were expressed at detectable and comparable levels in the total cell lysates (Fig. 2b, lower panels). These results suggest that the β2-β3-α2-β4-α3 regions, which are known to be important in $G\alpha_q$ for PLCβ interaction, might not be sufficient for $G\alpha_{14}$ to interact with PLCβ.

The co-immunoprecipitation results were subsequently confirmed by PLCβ functional assays. HEK293 cells were transfected with pcDNA1, $G\alpha_{14}$, $G\alpha_z$, the various chimeras or their constitutively active mutants and then subjected to IP_3 accumulation assay. In agreement with previous reports [24, 30], expression of $G\alpha_{14}$QL but not $G\alpha_z$QL significantly stimulated IP_3 formation (Fig. 2c). Both 14z151QL and 14z173QL also stimulated IP_3 production whereas 182z14QL and 203z14QL failed to do so (Fig. 2c). None of the wild-type chimeras significantly affected IP_3 production as compared to the vector controls (results not shown). Hence, these results demonstrate that the mere presence of the β2-β3-α2-β4-α3 regions of $G\alpha_{14}$ does not necessarily confer upon the Gα subunit an ability to stimulate PLCβ. More interestingly, these regions can be functionally replaced by those from $G\alpha_z$.

To test if the replacement of the PLC-interacting regions of $G\alpha_{14}$ by cognate sequences from $G\alpha_z$ can indeed support PLCβ activation, we swapped the β2-β3 or the α2-β4-α3 regions independently between the two Gα subunits (Fig. 3a). Among the various PLC-interacting regions, the α2 and α3 helices harbor most of residues that have been identified to form intermolecular bonds

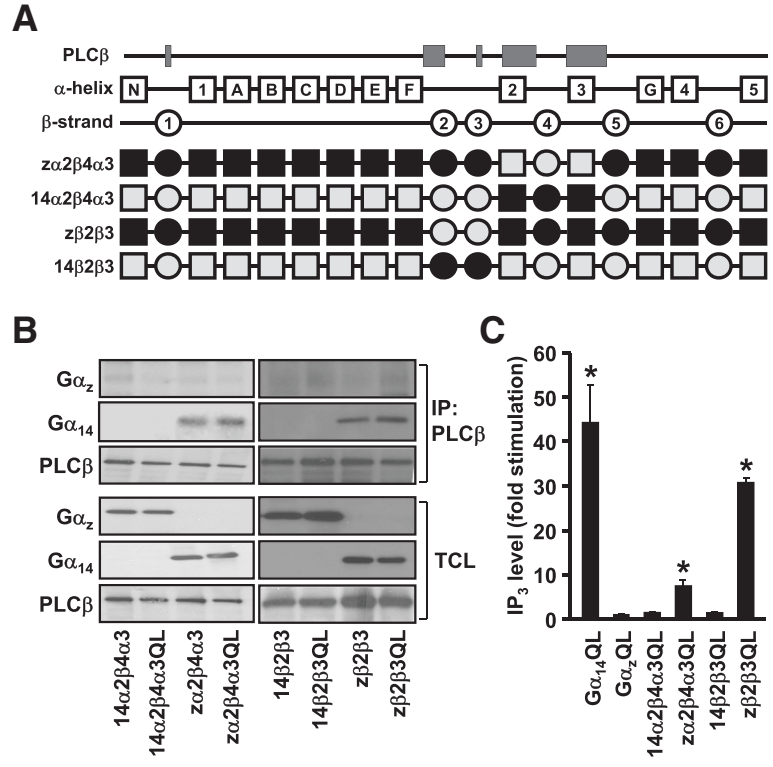

Fig. 3 Role of β2-β3 and α2-β4-α3 regions of $G\alpha_{14}$ in interaction and activation of PLCβ. **a** Schematic representation of zα2β4α3, 14α2β4α3, zβ2β3 and 14β2β3 chimeras. **b**, Cells were co-transfected with PLCβ2 and Gα protein or the indicated chimeras. Co-immunoprecipitation assays were performed and analyzed as in Fig. 2. Data shown represent one of three sets of immunoblots; two other sets yielded similar results. **c** HEK293 cells were transiently transfected with the wild-type or constitutively active mutants (QL) of Gα proteins or chimeras and then subjected to IP_3 accumulation assay and analyzed as in Fig. 2. *, IP_3 production was significantly enhanced as compared to corresponding wild-type transfected cells; Dunnett *t* test, $p < 0.05$

with PLCβ3 (Fig. 1a; [13]). Hence, substitution of the α2-β4-α3 regions in $G\alpha_{14}$ with those of $G\alpha_z$ might severely disrupt the ability of the resultant chimera (named as zα2β4α3) to interact with PLCβ. Although zα2β4α3 was co-immunoprecipitated by anti-PLCβ2 (Fig. 3b), its constitutively active mutant displayed a much weaker ability to induce IP_3 formation as compared to $G\alpha_{14}$QL (Fig. 3c). In contrast, chimera 14α2β4α3 (the mirror image of zα2β4α3) failed to associate or stimulate PLCβ2, suggesting that the α2-β4-α3 of $G\alpha_{14}$ alone was insufficient to ensure PLCβ interaction. Likewise, we examined the role of the β2-β3 strands of $G\alpha_{14}$ in PLCβ interaction. Chimera of $G\alpha_{14}$ with the β2-β3 domain replaced by $G\alpha_z$ (zβ2β3), and its mirror image (14β2β3), were constructed to determine if β2-β3 alone would affect PLCβ interaction with $G\alpha_{14}$ (Fig. 3a). Our results showed that zβ2β3 remained capable of interacting with PLCβ and stimulating its activity (Fig. 3b, c), suggesting that the $G\alpha_z$-specific residues in this region are sufficiently similar to those of $G\alpha_{14}$ to allow productive interaction with PLCβ. On the other hand, 14β2β3 with most of the C-terminal and N-terminal of $G\alpha_{14}$ replaced by $G\alpha_z$, failed to interact with PLCβ2 or mediate IP_3 production (Fig. 3b, c).

The N-terminal helical domain of $G\alpha_{14}$ is important for PLCβ interaction and activation

The preceding results suggested that the N-terminal half (αN-αF) of $G\alpha_{14}$ is seemingly important for PLCβ interaction and activation. Substituting the N-terminal of $G\alpha_{14}$ from αN to αF with $G\alpha_z$ completely abolished the ability of $G\alpha_{14}$ to activate PLCβ even though the chimeras (182z14 and 203z14) can be successfully expressed (Fig. 2). To narrow down the residues in αN-αF which are involved in PLCβ activation, the N-terminal helical domain (αA-αF) of $G\alpha_{14}$ was split into two halves and replaced by cognate sequences from $G\alpha_z$ (Fig. 4a). The helical domain is essential for maintaining the overall structure of the Gα subunit and participates in effector regulation [31]. In order to minimize possible disruption to the Gα structure, the chimeras were designed to switch from $G\alpha_{14}$ to $G\alpha_z$ or vice versa at a position in the middle of the helical domain (Fig. 4a) where the residues of the two templates have high homology. Chimera 14z224 harboring the αN-αC of $G\alpha_{14}$ was expressed efficiently but was unable to functionally associate with PLCβ (Fig. 4b, c). The mirror image of 14z224, chimera 131z14, also failed to interact with PLCβ or stimulate IP_3 formation (Fig. 4b, c). Replacement of the

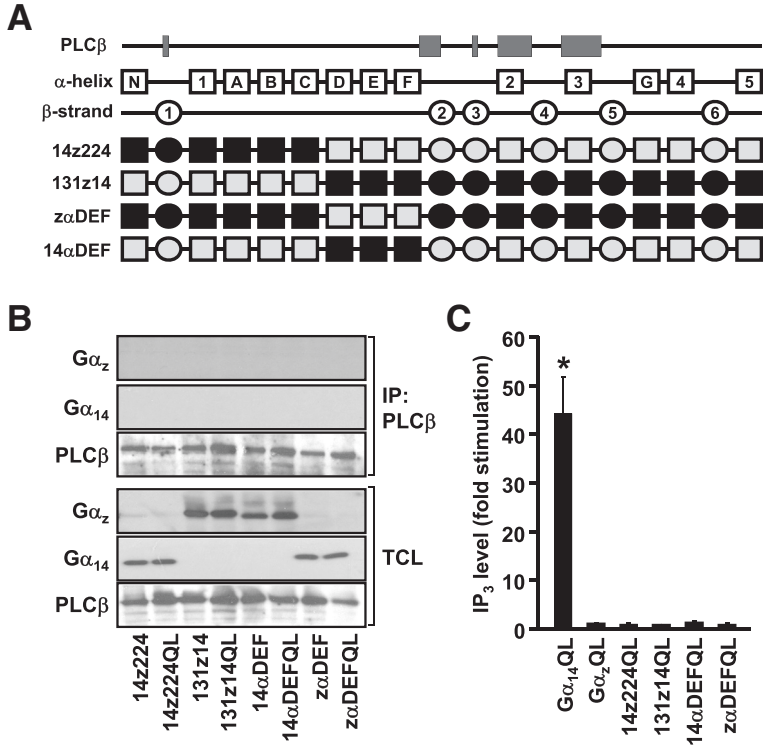

Fig. 4 An intact N-terminal and helical domain are required for $G\alpha_{14}$ mediated PLCβ interaction and activation. **a** Schematic representation of the 14z224, 131z14, 14αDEF and zαDEF chimeras. **b**, Cells were co-transfected with PLCβ2 and the indicated chimeras. Co-immunoprecipitation assays were performed and analyzed as in Fig. 2. Data shown represent one of three sets of immunoblots; two other sets yielded similar results. **c** HEK293 cells were transiently transfected with the wild-type or constitutively active mutants (QL) of Gα protein or the indicated chimeras and then subjected to IP_3 accumulation assay and analyzed as in Fig. 2. *, IP_3 production was significantly enhanced as compared to corresponding wild-type transfected cells; Dunnett *t* test, $p < 0.05$

second half of the helical domain (αD-αF) of $G\alpha_{14}$ by $G\alpha_z$ sequences, or vice versa, produced chimeras zαDEF and 14αDEF that neither interacted with PLCβ nor stimulated IP_3 formation (Fig. 4b, c). It should be noted that chimeras 131z14 and zαDEF contained the putative PLCβ-interacting core domain (Fig. 4a).

The extreme N-terminus of the Gα subunit contains motifs for membrane localization and is thus often removed prior to crystallization [13]. By superimposing the N-terminal αN helix onto the crystal structure of $G\alpha_q$, molecular modeling of the $G\alpha_q$/PLCβ3 complex predicts that the αN helix may represent a contact site for PLCβ3 (Fig. 5a). Given that several chimeras (14z151, 14z173, zα2β4α3 and zβ2β3) were able to stimulate PLCβ activity despite having the PLCβ-interacting core region from $G\alpha_z$, the provision of a $G\alpha_{14}$ αN helix on a $G\alpha_z$ backbone (14αN) might allow the resulting chimera to interact with PLCβ. However, chimera 14αNQL (Fig. 5b) did not stimulate IP_3 formation whereas chimera zαNQL ($G\alpha_{14}$ backbone with a $G\alpha_z$αN helix) functionally interacted with PLCβ (Fig. 5c). Collectively, these results suggest that the αN helix is not a critical determinant in the recognition of PLCβ by $G\alpha_{14}$.

Non-PLCβ-interacting $G\alpha_{14}$ chimeras can interact with other effectors

Since nine chimeras (181z14, 203z14, 14α2β4α3, 14β2β3, 14z224, 131z14, zαDEF, 14αDEF, and 14αN) failed to interact with PLCβ despite clear evidence of expression, we sought to determine if these chimeric Gα subunits were in fact functional. Those chimeras harboring large segments of $G\alpha_z$ sequence may behave like $G\alpha_z$ and thus be capable of inhibiting adenylyl cyclase. The panel of chimeras was therefore subjected to cAMP accumulation assay. The ability of the constitutively active mutant of each chimera to inhibit forskolin-induced cAMP accumulation was compared to its corresponding wild-type chimera (Fig. 6a). Like $G\alpha_z$QL, the constitutively active mutants of 14β2β3, 14z224, 14αDEF, and 14αN inhibited the forskolin response by 55-80 %, thereby confirming that these chimeras can adopt an active conformation. With four of the nine non-PLCβ-interacting chimeras demonstrating an ability to inhibit adenylyl cyclase, only five chimeras remained functionally unaccounted for.

Apart from being able to stimulate PLCβ by direct association [32, 33], $G\alpha_{14}$ can also activate the Ras/ERK signaling pathway by interacting with TPR1 [34]. The Gα/TPR1 interaction is important for IKK and STAT3 phosphorylation via the Ras/ERK pathway [35, 36] and is apparently independent of PLCβ [25]. Since five chimeras (203z14, 182z14, 131z14, zαDEF, and 14α2β4α3) failed to exhibit any functional response in either IP_3 or cAMP accumulation assays, we tested if these chimeras can associate with TPR1. HEK293 cells were co-transfected with an N-terminal Flag-tagged TPR1 (Flag-TPR1) and either the wild-type or the constitutively active mutant of $G\alpha_{14}$, $G\alpha_z$, or a chimera. Transfectants were subjected to co-immunoprecipitation using an anti-Flag affinity gel and protein G sepharose. The immunoprecipitates and cell lysates were then examined by western blot analysis using anti-Flag and either anti-$G\alpha_{14}$ or anti-$G\alpha_z$ antisera, depending on whether the N-terminus of the chimera is made up of $G\alpha_{14}$ or $G\alpha_z$ sequences. In agreement with previous studies [25, 34], neither $G\alpha_z$ nor $G\alpha_z$QL interacted with Flag-TPR1 whereas both $G\alpha_{14}$ and $G\alpha_{14}$QL co-immunoprecipitated with Flag-TPR1; noticeably more $G\alpha_{14}$QL was associated with Flag-TPR1 (Fig. 6b). In contrast to $G\alpha_z$, chimeras 203z14, 182z14, 131z14, and 14α2β4α3 were clearly detectable in the Flag-TPR1 immunoprecipitates (Fig. 6b); TPR1 interaction with 14α2β4α3 appeared to be weaker than the other chimeras. However, zαDEF could not be co-immunoprecipitated by Flag-TPR1 (Fig. 6b). Hence, only zαDEF did not exhibit any response in all of the functional assays. The ability of other chimeras to interact with Flag-TPR1 was similarly examined (Additional file 1: Figure S3) and the results are summarized in Table 1. Besides the inability of zαDEF to interact with Flag-TPR1, 14β2β3 and 14αN also exhibited negligible association with Flag-TPR1 but they were capable of coupling to adenylyl cyclase (Fig. 6a).

Results obtained from the various assays are summarized in Table 1. Collectively, these results suggest that the core PLCβ-interacting regions are insufficient to ensure productive interaction with PLCβ and, more surprisingly, some of these regions can be functionally substituted by cognate residues from $G\alpha_z$. Interestingly, an intact N-terminal helical domain (αA-αF) of $G\alpha_{14}$ are seemingly important for $G\alpha_{14}$-mediated PLCβ activation. $G\alpha_{14}$ chimeras with αA-αF replaced entirely or in part by $G\alpha_z$ can be expressed at a detectable level but failed to interact with PLCβ2 or stimulate IP_3 production.

Discussion

Structure and function correlations of members within the same protein family are often based on extensive analyses of a prototypical member. In the case of the $G\alpha_q$ family, it is generally assumed that all members interact with the canonical effector PLCβ in much the same way as $G\alpha_q$. The biochemical functions of $G\alpha_q$ family members are almost indistinguishable [33, 37] except for their ability to recognize specific receptors [38]. Hence, it is rather surprising that the putative PLCβ-interacting domains identified from studies on $G\alpha_q$ [13, 14, 17, 39] are simply insufficient to support efficient regulation of PLCβ by $G\alpha_{14}$. Although detailed structural comparison between $G\alpha_q$ and $G\alpha_{14}$ is not feasible because of the lack of $G\alpha_{14}$ structural data, the overall sequence similarity of over 80 % indicates a highly conserved three-dimensional

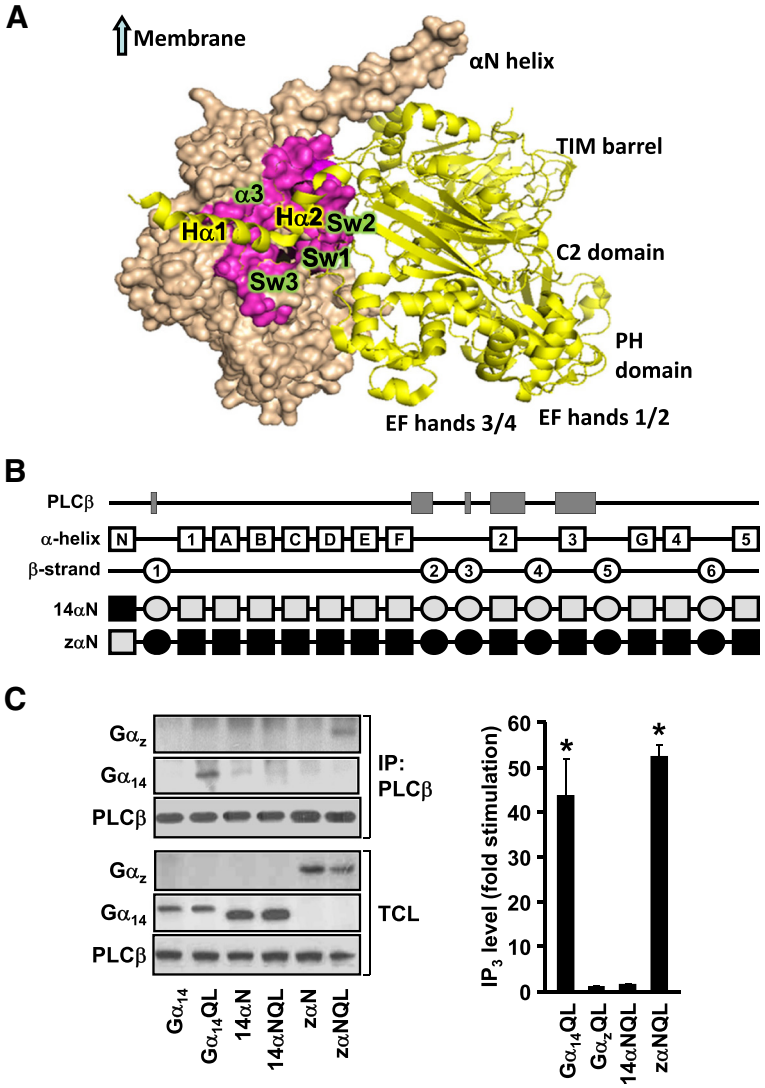

Fig. 5 Role of the N-terminal helix (α_N) in the $G\alpha_q$-PLCβ3 complex. **a** The model of $G\alpha_q$ (light orange) is shown as a space filling structure and contains the α_N-helix and other regions as indicated. PLCβ3 (yellow) is depicted as a cartoon ribbon, containing the helix-turn-helix segment (Hα1/Hα2), the N-terminal PH domain, four EF hands, the catalytic TIM barrel, and a C2 domain. PLCβ3-interacting residues of $G\alpha_q$ are colored in magenta. The carboxy-terminal (CT) domain of PLCβ3 is not included in the structural model. The structure of the α_N-helix is generated by replacing the amino acid sequence of $G\alpha_i$ ($G\alpha_i\beta_1\gamma_2$, PDB code: 1GP2) with the $G\alpha_q$ sequence. The final model is generated by alignment of $G\alpha_q$-PLCβ3 (PDB code: 3OHM) and the modified heterotrimer $G\alpha_q\beta_1\gamma_2$ using PyMOL (The PyMOL Molecular Graphics System, Version 1.3 Schrödinger, LLC). The orientation of the α_N-helix represents the conformation in the heterotrimer and is not optimized for the $G\alpha_q$-PLCβ3 complex. In this case, the α_N-helix points towards the cell membrane and clashes with PLCβ3, but in fact may exist in a conformation which interacts with PLCβ3. **b** Schematic representation of 14αN and zαN chimeras. **c** Cells were co-transfected with PLCβ2 and Gα protein or the indicated chimeras. Co-immunoprecipitation assays were performed and analyzed as in Fig. 2. Data shown represent one of three sets of immunoblots; two other sets yielded similar results. For the IP_3 accumulation assay, HEK293 cells were transiently transfected with the wild-type or constitutively active mutants (QL) of Gα proteins or chimeras and analyzed as in Fig. 2. *, IP_3 production was significantly enhanced as compared to corresponding wild-type transfected cells; Dunnett *t* test, $p < 0.05$

structure shared by both proteins [18, 19]. Since the structural homology and the residues responsible for PLCβ interaction and activation are presumably conserved from $G\alpha_q$ to $G\alpha_{14}$, one would expect that $G\alpha_{14}$ may utilize the same residues for PLCβ activation. It should also be noted that sequence variations in interacting residues of PLCβ2 and PLCβ3 may affect the ability of $G\alpha_{14}$ to efficiently stimulate PLCβ2. In particular, conservative substitutions such as D973E and Q1066S in the distal CTD may have limited consequences for $G\alpha_{14}$ binding, whereas more severe mutations in other interacting regions (E261S, Y855L, and R1062A) may significantly affect efficient activation by Gα proteins. Nonetheless, the substantial amount of conserved $G\alpha_q$-interacting residues (76 %) in PLCβ2 should

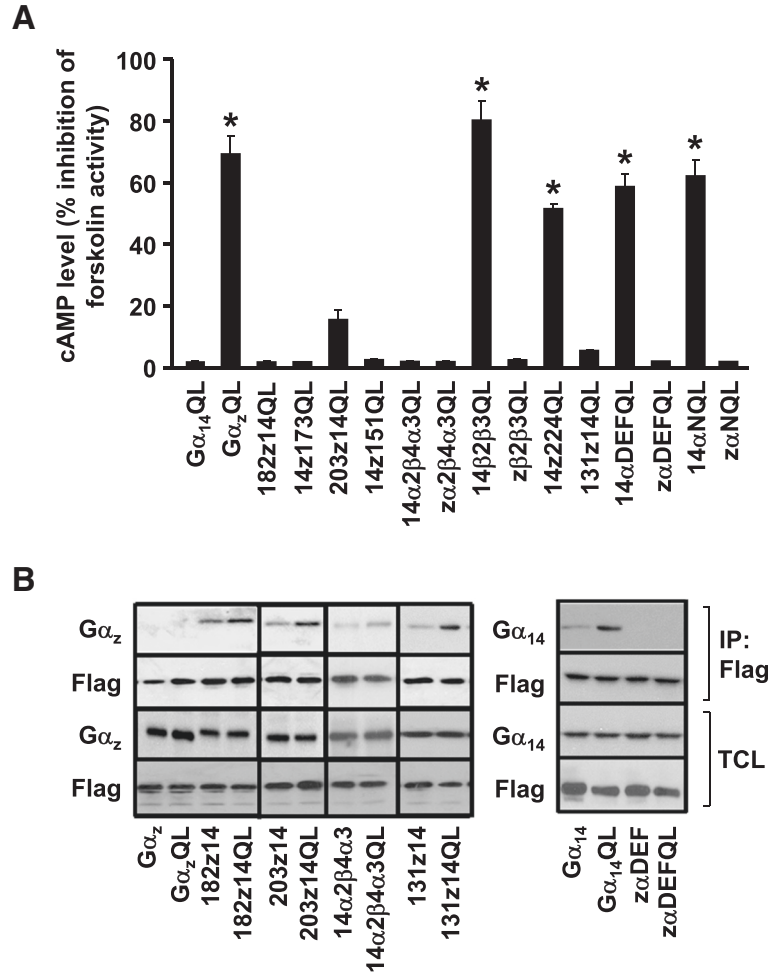

Fig. 6 Ability of different chimeras to interact with AC and TPR1. **a** HEK293 cells were transiently transfected with the wild-type or constitutively active mutants of Gα protein and chimeras indicated in the figure. The transfectants were labelled with [^{3}H]adenine (1 μCi/ml) in 1 % FBS/MEM. The labelled cells were treated with 50 μM of FSK for 30 min before subjected to cAMP accumulation assay. cAMP fold inhibition was calculated as the ratios of QL-induced to wild-type cAMP inhibition. Data represent the mean ± S.E.M. of three independent experiments, $n = 3$. *, cAMP accumulation was significantly inhibited as compared to corresponding wild-type transfected cells; Dunnett t test, $p < 0.05$. **b** HEK293 cells were transiently co-transfected with FLAG-TPR1 in combination with Gα proteins and the indicated chimeras. Cell lysates were immunoprecipitated by anti-FLAG affinity agarose gel. The immunoprecipitates were immunoblotted with anti-$G\alpha_{14}$, anti-$G\alpha_z$ or anti-FLAG antiserum. Crude lysates were used to examine the expression levels of $G\alpha_{14}$, $G\alpha_z$, $G\alpha_{14}/G\alpha_z$ chimeras or FLAG-TPR1 by Western blot analysis. The immunoblots shown represent one of three sets of immunoblots; two other sets yielded similar results

provide sufficient interacting regions for effector activation. However, $G\alpha_{14}/G\alpha_z$ chimeras lacking the putative PLCβ interacting domain (e.g., 14z151 and 14z173) are fully capable of interacting and stimulating PLCβ. Since these gain-of-function results do not correspond with current structural information on $G\alpha_q$/PLCβ interaction [13, 14], it would appear that our understanding on how G proteins stimulate the PLCβ pathway is far from complete.

$G\alpha_{14}$ and $G\alpha_q$ resemble each other both structurally and biochemically. Both proteins are able to stimulate PLCβ2 and exhibit similar profiles of IP_3 production [32]. Similar to other members of the $G\alpha_q$ subfamily, $G\alpha_{14}$ links a variety of G_q-, G_s-, and G_i- coupled receptors to stimulate PLCβ3 [40–42]. In addition, palmitoylation of cysteine residues in the N termini of $G\alpha_q$ and $G\alpha_{14}$ is essential for membrane localization and efficient PLCβ activation [43, 44]. However, co-immunoprecipitation and PLCβ activation studies using $G\alpha_{14}/G\alpha_z$ chimeras suggested that an intact helical domain (αN-αF) of $G\alpha_{14}$, but not the previously identified PLCβ3 interacting regions (α2-β4-α3-β5), is required for PLCβ interaction and activation. It should be noted that each Gα protein can be divided into the GTPase domain that comprises the PLCβ interacting regions and the helical domains composed of αA to αF

Table 1 Functional characterizations of the chimeras and their correlation with intact PLCβ or $G\alpha_{14}$ helical domains

	PLCβ stimulation	Adenylyl cyclase inhibition	PLCβ interaction	TPR1 interaction	Intact PLCβ domain	Intact $G\alpha_{14}$ helical domain
$G\alpha_{14}$	Yes	No	Yes	Yes	Yes	Yes
203z14	No	No	No	Yes	Yes	No
14z151	Yes	No	Yes	Yes	No	Yes
182z14	No	No	No	Yes	Yes	No
14z173	Yes	No	Yes	Yes	No	Yes
14β2β3	No	Yes	No	No	No	No
zβ2β3	Yes	No	Yes	Yes	Yes	Yes
14z224	No	Yes	No	Yes	No	No
131z14	No	No	No	Yes	Yes	No
14αDEF	No	Yes	No	Yes	No	No
zαDEF	No	No	No	No	Yes	No
14α2β4α3	No	Yes	No	Yes	No	No
zα2β4α3	Yes	No	Yes	Yes	No	Yes
14αN	No	Yes	No	No	No	No
zαN	Yes	No	Yes	Yes	Yes	Yes
$G\alpha_z$	No	Yes	No	No	No	No

Results of Gα proteins and chimeras in functional studies and co-immunoprecipitation assays are summarized. PLCβ stimulation was determined by measuring IP_3 production by constitutively active (QL) chimeras as compared to their corresponding wild type activity (Figs. 2c, 3c, 4c, and 5c). The ability of QL-chimeras to inhibit adenylyl cyclase was determined in FSK-induced cAMP accumulation assays (Fig. 6a). Co-immunoprecipitation assays were performed using anti-PLCβ2 and anti-FLAG for the detection of PLCβ (Figs. 2b, 3b, 4b, and 5c) and TPR1 (Fig. 6b), respectively. Constructs containing an intact PLCβ binding domain (α2-β4-α3-β5 region) or an intact helical domain (αA-αF region) of $G\alpha_{14}$ are also shown

helices [31]. There is increasing evidence to suggest that the helical domain participates in the activation and regulation of the Gα subunit [45]. For instance, the helical domain of $G\alpha_{16}$ is known to bind GRK2 [46]. Substitution of the previously identified PLCβ3 interacting regions (α2-β4-α3-β5) of $G\alpha_{14}$ by $G\alpha_z$ is expected to abolish PLCβ interaction and activation. However, $G\alpha_{14}/G\alpha_z$ chimeras consisting of varying combinations of the interacting regions were able to interact and activate PLCβ. Most surprisingly, the 14z151QL chimera, consisting of an entire α2-β4-α3-β5 region of $G\alpha_z$, was able to stimulate IP_3 production to similar levels as $G\alpha_{14}$, indicating that this region is not responsible for specifying interaction with PLCβ. The reduction in PLCβ activity of the 14z173QL chimera, consisting of an additional substitution of the adjacent β2-β3 region by $G\alpha_z$, could be caused by its weaker binding with PLCβ, as lower protein levels of the chimera were observed in complex with PLCβ in the co-immunoprecipitation assay (Fig. 2b). Also, a GTPase domain consisting of an intact α2-β4-α3-β5 region of either $G\alpha_{14}$ or $G\alpha_z$ seems important for maximal activation of PLCβ. The zα2β4α3QL chimera disrupts this region and decreased IP_3 production was observed without obvious binding defects as determined in the co-immunoprecipitation assay. In general, chimeras with substitutions in the GTPase domain of $G\alpha_{14}$ showed limited binding defects but significant effects on IP_3 production, which emphasizes the importance of the GTPase domain in PLCβ activation as compared to its less prominent role in protein binding.

Further co-immunoprecipitation and PLCβ activation studies using $G\alpha_{14}/G\alpha_z$ chimeras suggested that the helical domain of $G\alpha_{14}$ is required for PLCβ activation. Replacing either half (amino acids 1–131, or 132–181) of the N-terminus of $G\alpha_{14}$ by $G\alpha_z$ disrupted the ability of the chimeras (14z224, 131z14, zαDEF, and 14αDEF) to interact with PLCβ, suggesting that an intact helical core is necessary for PLCβ binding. To date, the sites for effector binding have been mostly mapped to the GTPase domain [13, 14, 17, 39, 47, 48], while much less is known about the function of the helical domain. The helical domain is the most divergent among Gα subunits [49]. Early structural and sequence analyses on Gα predicted that the helical domain is involved in effector interaction and may act as a regulatory entry point for GPCRs and Gβγ subunits [49, 50]. Together with the GTPase domain, it forms the nucleotide binding pocket and regulates GDP/GTP exchange by altering the binding affinity of Gα and its substrate [51, 52]. It has been proposed to participate in G protein oligomerization [53] and in the transition between the inactive and active conformations of Gα [54]. Furthermore, the helical domain of $G\alpha_s$ has been proposed to accelerate GTP hydrolysis by the GTPase domain, functioning as a GTPase-activating protein (GAP) [55]. A study using human/*Xenopus* chimeras of $G\alpha_s$ subunit revealed that the helical domain of $G\alpha_s$ is also important for

the activation of adenylyl cyclase [56]. More recently, crystallization studies suggest that major displacement of the helical domain is required for receptor coupling [57], thereby proposing a role for the helical domain as the inhibitory barrier for receptor-dependent activation. Considering the potential functions of the helical domain, our present study supports the involvement of the helical domain in effector interaction and regulation.

According to recent structural data, the αN helix is an important structure of Gα subunits in many aspects [14]. It is required for the binding of Gβγ [58, 59] and GPCRs [27, 60, 61]. It is also the site of lipid modification which enables proper localization of the G proteins to the plasma membrane (reviewed in [62]). Truncation of the αN helix of $G\alpha_q$ decreased $G\alpha_q$-stimulated PLCβ3 activity without affecting the binding affinity (K_i) with PLCβ3 [14]. Likewise, mutations in the hydrophobic surface of the distal CTD of PLCβ3, which is thought to form interactions with the αN helix of $G\alpha_q$, did not decrease the binding affinity while IP_3 production was still observed at considerable levels [14]. Consistently, our zαNQL chimera with the αN helix of $G\alpha_{14}$ replaced by $G\alpha_z$ did not show binding defects in co-immunoprecipitation assays and successfully induced IP_3 production. Moreover, removal of the distal CTD domain of PLCβ3 has been shown to significantly inhibit IP_3 production while only modestly affecting the binding affinity with $G\alpha_q$ [14]. These results suggest that interaction between the distal CTD of PLCβ3 and the αN helix of $G\alpha_q$ or $G\alpha_{14}$ is important for maximal stimulation of PLCβ3 and plays a less prominent role in Gα protein binding.

$G\alpha_z$ belongs to the $G\alpha_i$ subfamily and is able to inhibit adenylyl cyclase (AC) activity and subsequent cAMP production by direct association with AC (Fig. 6). Accordingly, substitution of $G\alpha_z$ by portions of $G\alpha_{14}$ structure may affect the level of inhibition of cAMP production. Disruption of the GTPase domain of $G\alpha_z$, as demonstrated by the 14α2β4α3 chimera, abolishes the ability of $G\alpha_z$ to inhibit AC. The 14z224QL chimera significantly inhibited cAMP production as compared to 14z173QL, which lacks the αDEF region of $G\alpha_z$ and was unable to inhibit AC. However, the 14αDEFQL chimera with an αDEF region of $G\alpha_q$ significantly inhibited AC at comparable levels. Moreover, chimeras lacking the entire helical domain of $G\alpha_z$ (14z151 and 14z173) were unable to inhibit AC. These results suggest that both an intact GTPase domain of $G\alpha_z$, which agrees with previously reported literature [39, 48], and at least a portion of the helical domain of $G\alpha_z$ is required for AC inhibition.

$G\alpha_{14}$ and $G\alpha_{16}$ belong to the same family and share high homology in terms of their amino acid sequence and signaling properties. Both $G\alpha_{14}$ and $G\alpha_{16}$ have been shown to activate Ras and downstream transcription factors such as NFκB and STAT3 through interaction with TPR1 [25, 34]. Previous studies using $G\alpha_{16}/G\alpha_z$ chimeras suggested that the β2 and β3 strands of $G\alpha_{16}$ are important for the interaction with TPR1 but this is not necessarily the case for $G\alpha_{14}$. Co-immunoprecipitation studies using $G\alpha_{14}/G\alpha_z$ chimeras (summarized in Table 1) suggest that TPR1 interacts with $G\alpha_{14}$ and $G\alpha_{16}$ through different structural regions. As demonstrated by the zαDEF chimera, the αDEF region of $G\alpha_{14}$ seems necessary for interaction with TPR1. However, several chimeras lacking this region, including 182z14, 203z14, and 131z14, are able to interact with TPR1. The inability of the zαDEF chimera to interact with TPR1 could be caused by disruption of the helical domain resulting in instability of the protein structure. Disruption of the GTPase domain and substitution of the helical domain by $G\alpha_z$, as demonstrated by the zα2β4α3 chimera, did not completely abolish TPR1 interaction. Moreover, the mirror image pairs 14z151 and 203z14, as well as 14z173 and 182z14, were able to interact with TPR1. These results indicate that the presence of either the α2-β4-α3 region of the GTPase domain or an intact helical domain of $G\alpha_{14}$ is sufficient for TPR1 interaction.

Conclusion

The present study has successfully used chimeric $G\alpha_{14}/G\alpha_z$ constructs to map critical regions for effector regulation and demonstrates the insufficiency of previous structural information in supporting efficient effector regulation by Gα proteins. Although the roles of the αN helix and helical domain of Gα subunits in G protein-mediated signal transduction have mostly been neglected, our results designate important roles for these domains of $G\alpha_{14}$ in effector interaction and activation.

Methods

Reagents

The human cDNAs of $G\alpha_{14}$, $G\alpha_{14}$QL were obtained from Guthrie Research Institute (Sayre, PA, USA). Cell culture reagents, including LipofectAMINE PLUS reagents, and Lipofectamin 2000 were purchased from Invitrogen (Carlsbad, CA, USA). Anti-$G\alpha_{14}$ targeting the N-terminal was obtained from Gramsch Laboratories (Schwabhausen, Germany). Anti-FLAG antibody and anti-FLAG affinity gel were from Sigma-Aldrich (St. Louis, MO, USA). Other antibodies were purchased from Cell Signaling Technology (Danvers, MA, USA). Protein G-agarose and dithiobis[succinimidylpropionate] (DSP) cross-linker were from Pierce Biotechnology (IL, USA). Osmonics nitrocellulose membrane and ECL kit were from Westborough (MA, USA) and Amersham (Piscataway, NJ, USA), respectively. Pertussis toxin (PTX) was obtained from List Biological Laboratories (Campbell, CA, USA), and octreotide (OCT) was from Sigma-Aldrich (St. Louis, MO, USA).

Cell culture and co-immunoprecipitation

HEK293 cells were obtained from the American Type Culture Collection (CRL-1573, Rockville, MD). They were maintained in Eagle's minimum essential medium at 5 % CO_2, 37 °C with 10 % fetal bovine serum, 50 units/mL penicillin and 50 μg/mL streptomycin. For co-immunoprecipitation experiments, HEK293 cells were grown to 80 % confluency in 100 mm tissue culture plates and then co-transfected with 200 ng Gα and 200 ng FLAG-TPR1 cDNAs using 15 μL PLUS and LipofectAMINE reagents in Opti-MEM. Serum was replenished 3 h after transfection. Cross-linking was performed one day after transfection; transfected HEK293 cells were washed with PBS twice and then treated with 0.5 mM DSP in PBS for 15 min at room temperature. Cells were then washed again with PBS and maintained in quenching solution (50 mM glycine in PBS, pH 7.4) for 5 min. Subsequently, cells were lysed in ice-cold RIPA buffer (25 mM HEPES at pH 7.4, 0.1 % SDS, 1 % Nonidet P-40, 0.5 % sodium deoxycholate, 1 mM dithiothreitol, 200 μM Na_3VO_4, 4 μg/mL aprotinin,100 μM phenylmethylsulfonyl fluoride, and 2 μg/mL leupeptin). Cell lysates were gently rocked with an anti-$G\alpha_{14}$ antiserum at 4 °C overnight, and then incubated in 30 μL protein G-agarose (50 % slurry) at 4 °C for 2 h. Alternatively, the cell lysates were incubated in 30 μL anti-FLAG affinity agarose gel (50 % slurry) at 4 °C overnight. Immunoprecipitates were washed with ice-cold RIPA buffer (400 μL) for four times, resuspended in 50 μl RIPA buffer and 10 μl 6× sample buffer and then boiled for 5 min. $G\alpha_{14}$ and FLAG-TPR1 proteins in the immunoprecipitates were analyzed by Western blots.

Construction of chimeras

Gα chimeras were constructed from cDNAs encoding human $G\alpha_{14}$ and $G\alpha_z$ by using polymerase chain reaction (PCR) techniques. The N-terminal 37, 131, 182 and 203 residues of $G\alpha_{14}$ were substituted by the corresponding amino acids of $G\alpha_z$ to generate zαN, 131z14, 182z14 and 203z14 chimeras, respectively. Primers were designed to produce two half-length fragments with overlapping regions; the forward fragment was generated with the antisense and T7 primers, whereas the backward fragment was made with the sense and reverse primers which target a BGH polyadenylation signal (BGH primers). The two half-products were then annealed together to generate a full-length fragment by another round of PCR using T7 and BGH primers. Mirror images of these constructs were generated analogously and were named 14αN, 14z224, 14z173 and 14z151 chimeras. PCR (30 cycles each with 94 °C for 60 s, 58 °C for 60 s and 72 °C for 90 s) was carried out using AccuPrime PCR mix. The 14β2β3 chimera was constructed using 182z14 as the DNA template for the forward half-product and 14z151 DNA template for the backward half-product. The zβ2β3 chimera was constructed using 14z173 as the DNA template for the forward half-product and 203z14 as the DNA template for the backward half-product. 14α2β4α3 was constructed using 203z14 as the template for the forward half product and $G\alpha_z$ as the template for the backward half product. Its mirror image zα2β4α3 was constructed using 14z151 as the template for the forward half product and $G\alpha_{14}$ for the backward half product. Finally, 14αDEF was constructed using 131z14 as the DNA template for the forward half-product and $G\alpha_z$ as template for the backward half-product. Its mirror image zαDEF was constructed using 14z224 as the DNA template for the forward half-product and $G\alpha_{14}$ as template for the backward half-product. Primers for chimera construction are listed in Table 2. All Gα chimeras were checked by restriction mapping and then subcloned into pcDNA3 at *Hind*III and *Xba*I sites. The constructs were confirmed by dideoxynucleotide sequencing using Applied Biosystem Big Dye Terminator v3.1 Cycle Sequencing Kits (Foster City, CA, USA).

Inositol Phosphates (IP_3) accumulation assay

HEK293 cells were seeded on a 12-well plate at 2×10^5 cells/well one day prior to transfection. Cells were then transfected with 200 ng Gα using 2 μL PLUS and Lipofectamine reagents in Opti-MEM. On the next day, cells were labeled with inositol-free Dubecco's modified Eagle's medium (DMEM; 750 μL) containing 5 % FBS and 2.5 μCi/mL *myo*-[^{3}H]inositol overnight. Labeled cells were washed twice with the inositol phosphates assay medium (DMEM buffered with 20 mM HEPES, pH 7.5 and 5 mM LiCl) and were incubated for 1 h at 37 °C. Reactions were stopped by replacing the assay medium with 750 μL ice-cold 20 mM formic acid and the lysates were kept in 4 °C for 30 min before the separation of [^{3}H]IP from other labeled species by sequential ion-exchange chromatography as described previously [63].

cAMP accumulation assay

HEK293 cells were labeled overnight with [^{3}H]adenine (1 μCi/ml) in culture medium containing 1 % FBS. The labeled cells were rinsed once with 2 ml of assay medium (MEM containing 20 mM HEPES, pH 7.4) and incubated at 37 °C for 30 min with 1 ml of assay medium containing 1 mM 1-methyl-3-isobutylxanthine in the absence or presence of 50 μM forskolin. The cells were lysed with 1 ml 5 % trichloroacetic acid with 1 mM ATP to terminate the reaction and were stored at 4 °C for 1 h. Intracellular [^{3}H]cAMP was isolated by sequential chromatography as described previously [64]. The level of [^{3}H]cAMP was estimated by determining the ratios of [^{3}H]cAMP to total [^{3}H]ATP and [^{3}H]ADP pools.

Table 2 Primer sequences for constructing various $G\alpha_{14/z}$ chimeras

Chimera	Templates	Primers
203z14	$G\alpha_z/G\alpha_{14}$	F: 5′- ATGGTGGACGTGGGG***GGCCAACGATCGGAA*** -3′
		R: 5′- ***TTCCGATCGTTGGCC***CCCCACGTCCACCAT -3′
14z151	$G\alpha_{14}/G\alpha_z$	F: 5′- ***ATGGTGGATGTTGGT***GGGCAGAGGTCAGAG -3′
		R: 5′- CTCTGACCTCTGCCC***ACCAACATCCACCAT*** -3′
182z14	$G\alpha_z/G\alpha_{14}$	F: 5′- CGCTCCCGGGACATG***ACCACCGGCATCATT*** -3′
		R: 5′- ***ATTGATGCCGGTGGT***CATGTCCCGGGAGCG -3′
14z173	$G\alpha_{14}/G\alpha_z$	F: 5′- ***CGCGTCCGAGTGCCC***ACCACGGGCATTGTG -3′
		R: 5′- CACAATGCCCGTGGT***GGGCACTCGGACGCG*** -3′
14β2β3	182z14/14z151	F: 5′- ***ATGGTGGATGTTGGT***GGGCAGAGGTCAGAG -3′
		R: 5′- CTCTGACCTCTGCCC***ACCAACATCCACCAT*** -3′
zβ2β3	14z173/203z14	F: 5′- ATGGTGGACGTGGGG***GGCCAACGATCGGAA*** -3′
		R: 5′- ***TTCCGATCGTTGGCC***CCCCACGTCCACCAT -3′
14z224	$G\alpha_{14}/G\alpha_z$	F: 5′- ***GCCATCAAGCAGCTC***TGGGCCGACCCAGGG -3′
		R: 5′- CCCTGGGTCGGCCCA***GAGCTGCTTGATGGC*** -3′
131z14	$G\alpha_z/G\alpha_{14}$	F: 5′- GTCATGCGACGGCTC***TGGCAAGATCCAGGC*** -3′
		R: 5′- ***GCCTGGATCTTGCCA***GAGCCGTCGCATGAC -3′
14αDEF	131z14/$G\alpha_z$	F: 5′- ***CGCGTCCGAGTGCCC***ACCACGGGCATTGTG -3′
		R: 5′- CACAATGCCCGTGGT***GGGCACTCGGACGCG*** -3′
zαDEF	14z224/$G\alpha_{14}$	F: 5′- CGCTCCCGGGACATG***ACCACCGGCATCATT*** -3′
		R: 5′- ***AATGATGCCGGTGGT***CATGTCCCGGGAGCG -3′
14α2β4α3	203z14/$G\alpha_z$	F: 5′- ATGGTGGACGTGGGG***GGCCAACGATCGGAA*** -3′
		R: 5′- ***TTCCGATCGTTGGCC***CCCCACGTCCACCAT -3′
zα2β4α3	14z151/$G\alpha_{14}$	F: 5′- ***ATGGTGGATGTTGGT***GGGCAGAGGTCAGAG -3′ R: 5′- CTCTGACCTCTGCCC***ACCAACATCCACCAT*** -3′
14αN	$G\alpha_{14}/G\alpha_z$	F: 5′- ***GGGCAGAGGTCAGAG***CGCGAAATCAAGCTG -3′ R: 5′- CAGCTTGATTTCGCG***CTCTGACCTCTGCCC*** -3′
zαN	$G\alpha_z/G\alpha_{14}$	F: 5′- AGCCAGCGGCAACGC***CGTGAGCTTAAGCTG*** -3′ R: 5′- ***CAGCTTAAGCTCACG***GCGTTGCCGCTGGCT -3′

Bold and italic nucleotides denote the $G\alpha_{14}$-derived sequences. F, forward primer; R, reverse primer

Molecular modeling

$G\alpha_q$ in a complex with PLCβ3 (PDB ID: 3OHM, [13]) was employed to illustrate the interaction between Gα and PLCβ, and for creating a molecular model of $G\alpha_{14}$by homologous modeling using SWISS-MODEL [65, 66]. Visualization of various structures was accomplished using PyMOL (The PyMOL Molecular Graphics System, Version 1.3 Schrödinger, LLC).

Western blotting analysis

Protein samples were resolved on 12 % SDS-polyacrylamide gels and transferred to Osmonics nitrocellulose membrane. Resolved proteins were detected by their specific primary antibodies and horseradish peroxidase-conjugated secondary antisera. The immunoblots were visualized by chemiluminescence with the ECL kit from Amersham, and the images detected in X-ray films were quantified by densitometric scanning using the Eagle Eye II still video system (Stratagene, La Jolla, CA, USA).

Additional file

Additional file 1: Figure S1. Alignment of $G\alpha_q$-interacting residues in the PLCβ family. **Figure S2.** Alignment of PLCβ-interacting residues in the Gα protein family. **Figure S3.** Interaction of $G\alpha_{14}/G\alpha_z$ chimeras with Flag-TPR1. (PPTX 306 kb)

Abbreviations

AC: Adenylyl cyclase; ERK: Extracellular signal-regulated kinase; GPCRs: G protein-coupled receptors; HEK293: Human embryonic kidney 293; IP_3: Inositol trisphosphate; MAPK: Mitogen-activated protein kinase; PLCβ: Phospholipase Cβ; TPR1: Tetratricopeptide repeat 1.

Competing interests

The authors declare that they have no competing interests.

Authors' contributions

DHTK carried out most of the experiments and analyzed and interpreted the results. LYY performed several co-immunoprecipitation experiments. ASLC helped to design the mutant constructs and KMW performed molecular model constructions and participated in drafting the manuscript. YHW conceived the study and participated in its design and coordination as well as drafted the manuscript. All authors have read and approved the final version of the manuscript.

Acknowledgements
We thank Andy Liu, Cecilia Wong, and Joy Chan for helpful discussions. This work was supported in part by the National Key Basic Research Program of China (2013CB530900), Research Grants Council of Hong Kong (HKUST 660109), and the Hong Kong Jockey Club.
This work was supported in part by the National Key Basic Research Program of China (2013CB530900), Research Grants Council of Hong Kong (HKUST 660109), and the Hong Kong Jockey Club.

Received: 24 July 2015 Accepted: 26 August 2015
Published online: 16 September 2015

References

1. Oldham WM, Hamm HE. Heterotrimeric G protein activation by G-protein-coupled receptors. Nat Rev Mol Cell Biol. 2008;9(1):60–71.
2. Tesmer JJ. The quest to understand heterotrimeric G protein signaling. Nat Struct Mol Biol. 2010;17(6):650–2.
3. Sandal M, Paltrinieri D, Carloni P, Musiani F, Giorgetti A. Structure/function relationships of phospholipases C Beta. Curr Protein Pept Sci. 2013;14(8):650–7.
4. Jhon DY, Lee HH, Park D, Lee CW, Lee KH, Yoo OJ, et al. Cloning, sequencing, purification, and Gq-dependent activation of phospholipase C-beta 3. J Biol Chem. 1993;268(9):6654–61.
5. Lyon AM, Tesmer JJ. Structural insights into phospholipase C-β function. Mol Pharmacol. 2013;84(4):488–500.
6. Adjobo-Hermans MJ, Crosby KC, Putyrski M, Bhageloe A, van Weeren L, Schultz C, et al. PLCβ isoforms differ in their subcellular location and their CT-domain dependent interaction with Gαq. Cell Signal. 2013;25(1):255–63.
7. Berridge MJ, Irvine RF. Inositol trisphosphate, a novel second messenger in cellular signal transduction. Nature. 1984;312:315–21.
8. Ross E, Wilkie T. GTPase-activating proteins for heterotrimeric G proteins: regulators of G protein signaling (RGS) and RGS-like proteins. Annu Rev Biochem. 2000;69:795–827.
9. Dorn GW, Oswald KJ, McCluskey TS, Kuhel DG, Liggett SB. α_{2A}-adrenergic receptor stimulated calcium release is transduced by G_i-associated Gβγ-mediated activation of phospholipase C. Biochemistry. 1997;36:6415–23.
10. Park D, Jhon DY, Lee CW, Lee KH, Rhee SG. Activation of phospholipase C isozymes by G protein βγ subunits. J Biol Chem. 1993;268:4573–6.
11. Rozengurt E. Mitogenic signaling pathways induced by G protein-coupled receptors. J Cell Physiol. 2007;213(3):589–602.
12. Gaugler L, Raamsdonk CD V, Bezrookove V, Green G, Brien JMO, Simpson EM, et al. Frequent somatic mutations of GNAQ in uveal melanoma and blue naevi. Nature. 2009;457(7229):599–602.
13. Waldo GL, Ricks TK, Hicks SN, Cheever ML, Kawano T, Tsuboi K, et al. Kinetic scaffolding mediated by a phospholipase Cβ and G_q signaling complex. Science. 2010;330:974–80.
14. Lyon AM, Dutta S, Boguth CA, Skiniotis G, Tesmer JJG. Full-length $G\alpha_q$-phospholipase C-β3 structure reveals interfaces of the C-terminal coiled-coil domain. Nat Struct Mol Biol. 2013;20(3):355–62.
15. Park D, Jhon DY, Lee CW, Ryu SH, Rhee SG. Removal of the carboxyl-terminal region of phospholipase C-β1 by calpain abolishes activation by $G\alpha_q$. J Biol Chem. 1993;268:3710–4.
16. Kim CG, Park D, Rhee SG. The role of carboxyl-terminal basic amino acids in $G_q\alpha$-dependent activation, particulate association, and nuclear localization of phospholipase C-β1. J Biol Chem. 1996;271:21187–92.
17. Venkatakrishnan G, Exton J. Identification of determinants in the α-subunit of G_q required for phospholipase C activation. J Biol Chem. 1996;271:5066–72.
18. Wilkie TM, Scherle PA, Strathmann MP, Slepak VZ, Simon MI. Characterization of G-protein α subunits in the G_q class: expression in murine tissues and in stromal and hematopoietic cell lines. Proc Natl Acad Sci. 1991;88(22):10049–53.
19. Wilkie TM, Gilbert DJ, Olsen AS, Chen XN, Amatruda TT, Korenberg JR, et al. Evolution of the mammalian G protein α subunit multigene family. Nat Genet. 1992;1(2):85–91.
20. Conklin BR, Chabre O, Wong YH, Federman A, Bourne HR. Recombinant $G_{q\alpha}$: mutational activation and coupling to receptors and phospholipase C. J Biol Chem. 1992;267:31–4.
21. Hepler JR, Kozasa T, Smrcka AV, Simon MI, Rhee SG, Sternweis PC, et al. Purification from Sf9 cells and characterization of recombinant $G_q\alpha$ and $G_{11}\alpha$. Activation of purified phospholipase C isozymes by Gα subunits. J Biol Chem. 1993;268(19):14367–75.
22. Mody SM, Ho MK, Joshi SA, Wong YH. Incorporation of $G\alpha_z$-specific sequence at the carboxyl terminus increases the promiscuity of $G\alpha_{16}$ toward G_i-coupled receptors. Mol Pharmacol. 2000;57:13–23.
23. Tian YJ, New DC, Yung LY, Allen RA, Slocombe PM, Twomey BM, et al. Differential chemokine activation of CCR1-regulated pathways: selective activation of $G\alpha_{14}$-coupled pathways. Eur J Immunol. 2004;34:785–95.
24. Chan JSC, Lee JWM, Ho MKC, Wong YH. Preactivation permits subsequent stimulation of phospholipase C by G_i-coupled receptors. Mol Pharmacol. 2000;57:700–8.
25. Liu AMF, Lo RKH, Guo EX, Ho MKC, Ye RD, Wong YH. $G\alpha_{16}$ interacts with tetratricopeptide repeat 1 (TPR1) through its β3 region to activate Ras independently of phospholipase Cβ signaling. BMC Struct Biol. 2011;11:17.
26. Tsu RC, Ho MK, Yung LY, Joshi S, Wong YH. Role of amino- and carboxyl-terminal regions of $G\alpha_z$ in the recognition of G_i-coupled receptors. Mol Pharmacol. 1997;52(1):38–45.
27. Ho MK, Wong YH. The amino terminus of $G\alpha_z$ is required for receptor recognition, whereas its α4/β6 loop is essential for inhibition of adenylyl cyclase. Mol Pharmacol. 2000;58:993–1000.
28. Ho MK, Chan JH, Wong CS, Wong YH. Identification of a stretch of six divergent amino acids on the α5 helix of $G\alpha_{16}$ as a major determinant of the promiscuity and efficiency of receptor coupling. Biochem J. 2004;380(Pt 2):361–9.
29. Lo RKH, Wong YH. Signal transducer and activator of transcription 3 activation by the δ-opioid receptor via $G\alpha_{14}$ involves multiple intermediates. Mol Pharmacol. 2004;65:1427–39.
30. Yung LY, Joshi SA, Chan RYK, Chan JSC, Pei G, Wong YH. $G\alpha_{L1}$ ($G\alpha_{14}$) couples the ORL_1 receptor to stimulation of phospholipase C. J Pharmacol Exp Ther. 1999;288:232–8.
31. Liu W, Northup JK. The helical domain of a G protein α subunit is a regulator of its effector. Proc Natl Acad Sci U S A. 1998;95:12878–83.
32. Lee CH, Park D, Wu D, Rhee SG, Simon MI. Members of the Gq α subunit gene family activate phospholipase C β isozymes. J Biol Chem. 1992;267:16044–7.
33. Taylor S, Chae H, Rhee S, Exton J. Activation of the β1 isozyme of phospholipase C by α subunits of the G_q class of G proteins. Nature. 1991;350:516–8.
34. Kwan DHT, Yung LY, Ye RD, Wong YH. Activation of Ras-dependent signaling pathways by G_{14}-coupled receptors requires the adaptor protein TPR1. J Cell Biochem. 2012;113(11):3486–97.
35. Liu AMF, Lo RKH, Lee MMK, Wang Y, Yeung WWS, Ho MKC, et al. $G\alpha_{16}$ activates Ras by forming a complex with tetratricopeptide repeat 1 (TPR1) and Son of Sevenless (SOS). Cell Signal. 2010;22:1448–58.
36. Marty C, Browning DD, Ye RD. Identification of tetratricopeptide repeat 1 as an adaptor protein that interacts with heterotrimeric G proteins and the small GTPase Ras. Mol Cell Biol. 2003;23:3847–58.
37. Smrcka AV, Hepler JR, Brown KO, Sternweis PC. Regulation of polyphosphoinositide-specific phospholipase C activity by purified G_q. Science. 1991;251:804–7.
38. Lee CH, Shin IC, Kang JC, Koh HC, Ha JH, Min CJ. Differential coupling of $G\alpha_q$ family of G-protein to muscarinic M1 receptor and neurokinin-2 receptor. Arch Pharm Res. 1998;4:423–8.
39. Medina R, Grishina G, Meloni EG, Muth TR, Berlot CH. Localization of the effector-specifying regions of $G\alpha_{i2}$ and $G\alpha_q$. J Biol Chem. 1996;271:24720–7.
40. Ho MK, Yung LY, Chan JS, Chan JH, Wong CS, Wong YH. $G\alpha_{14}$ links a variety of G_i and G_s-coupled receptors to the stimulation of phospholipase C. Br J Pharmacol. 2001;132(7):1431–40.
41. Offermanns S, Simon MI. Gα15 and Gα16 couple a wide variety of receptors to phospholipase C. J Biol Chem. 1995;270(25):15175–80.
42. Kostenis E. Is Gα 16 the optimal tool for fishing ligands of orphan G-protein-coupled receptors? Trends Pharmacol Sci. 2001;22(11):560–4.
43. Linder ME, Middleton P, Hepler JR, Taussig R, Gilman AG, Mumby SM. Lipid modifications of G proteins: alpha subunits are palmitoylated. Proc Natl Acad Sci. 1993;90(8):3675–9.
44. Pedone KH, Hepler JR. The importance of N-terminal polycysteine and polybasic sequences for $G_{14}\alpha$ and $G_{16}\alpha$ palmitoylation, plasma membrane localization, and signaling function. J Biol Chem. 2007;282(35):25199–212.
45. Dohlman HG, Jones JC. Signal activation and inactivation by the Gα helical domain: a long-neglected partner in G protein signaling. Sci Signal. 2012;5(226):re2.
46. Day PW, Carman CV, Sterne-Marr R, Benovic JL, Wedegaertner PB. Differential interaction of GRK2 with members of the $G\alpha_q$ family. Biochemistry. 2003;42(30):9176–84.

47. Berlot CH, Bourne HR. Identification of effector-activating residues of $G\alpha_s$. Cell. 1992;68:911–22.
48. Grishina G, Berlot CH. Identification of common and distinct residues involved in the interaction of α_{i2} and α_s with adenylyl cyclase. J Biol Chem. 1997;272:20619–26.
49. Coleman DE, Berghuis AM, Lee E, Linder ME, Gilman AG, Sprang SR. Structures of active conformations of $G\alpha_{i1}$ and the mechanism of GTP hydrolysis. Science. 1994;265:1405–12.
50. Masters SB, Stroud RM, Bourne HR. Family of G protein α chains: amphipathic analysis and predicted structure of functional domains. Protein Eng. 1986;1:47–54.
51. Noel JP, Hamm HE, Sigler PB. The 2.2 A crystal structure of $\alpha_{transducin}$ complexed with GTPγS. Nature. 1993;366:654–63.
52. Remmers AE, Engel C, Liu M, Neubig RR. Interdomain interactions regulate GDP release from heterotrimeric G proteins. Biochemistry. 1999;38:13795–800.
53. Mixon MB, Lee E, Coleman DE, Berghuis AM, Gilman AG, Sprang SR. Tertiary and quaternary structural changes in $G\alpha_{i1}$ induced by GTP hydrolysis. Science. 1995;270:954–60.
54. Codina J, Birnbaumer L. Requirement for intramolecular domain interaction in activation of G protein α subunit by aluminum fluoride and GDP but not by GTPγS. J Biol Chem. 1994;269:29339–42.
55. Markby DW, Onrust R, Bourne HR. Separate GTP binding and GTPase activating domains of a G alpha subunit. Science. 1993;262(5141):1895–901.
56. Antonelli M, Birnbaumer L, Allende JE, Olate J. Human-Xenopus chimeras of $G\alpha_s$ reveal a new region important for its activation of adenylyl cyclase. FEBS Lett. 1994;340:249–54.
57. Rasmussen SG, DeVree BT, Zou Y, Kruse AC, Chung KY, Kobilka TS, et al. Crystal structure of the β_2 adrenergic receptor-G_s protein complex. Nature. 2011;477(7366):549–55.
58. Lambright DG, Sondek J, Bohm A, Skiba NP, Hamm HE, Sigler PB. The 2.0 A crystal structure of a heterotrimeric G protein. Nature. 1996;379:311–9.
59. Wall MA, Coleman DE, Lee E, Iniguez-Lluhi JA, Posner BA, Gilman AG, et al. The structure of the G protein heterotrimer $G\alpha_{i1}\beta_1\gamma_2$. Cell. 1995;83:1047–58.
60. Hamm HE, Deretic D, Arendt A, Hargrave PA, Koenig B, Hofmann KP. Site of G protein binding to rhodopsin mapped with synthetic peptides from the α subunit. Science. 1988;241:832–5.
61. Onrust R, Herzmark P, Chi P, Garcia PD, Lichtarge O, Kingsley C, et al. Receptor and βγ binding sites in the α subunit of the retinal G protein transducin. Science. 1997;275:381–4.
62. Marrari Y, Crouthamel M, Irannejad R, Wedegaertner PB. Assembly and trafficking of heterotrimeric G proteins. Biochemistry. 2007;46:7665–77.
63. Tsu RC, Chan JS, Wong YH. Regulation of multiple effectors by the cloned δ-opioid receptor: stimulation of phospholipase C and type II adenylyl cyclase. J Neurochem. 1995;64:2700–7.
64. Wong YH. G_i assays in transfected cells. Methods Enzymol. 1994;238:81–94.
65. Arnold K, Bordoli L, Kopp J, Schwede T. The SWISS-MODEL workspace: a web-based environment for protein structure homology modelling. Bioinformatics. 2006;22:195–201.
66. Bordoli L, Kiefer F, Arnold K, Benkert P, Battey J, Schwede T. Protein structure homology modelling using SWISS-MODEL Workspace. Nat Protoc. 2009;4:1.